TECHNICAL NOTE
D-859

UNSTEADY AERODYNAMIC FORCES ON A SLENDER BODY OF REVOLUTION IN SUPERSONIC FLOW

By Reuben Bond and Barbara B. Packard

Ames Research Center
Moffett Field, Calif.

NATIONAL AERONAUTICS AND SPACE ADMINISTRATION
WASHINGTON
May 1961

NATIONAL AERONAUTICS AND SPACE ADMINISTRATION

TECHNICAL NOTE D-859

UNSTEADY AERODYNAMIC FORCES ON A SLENDER BODY OF REVOLUTION IN SUPERSONIC FLOW

By Reuben Bond and Barbara B. Packard

SUMMARY

Linearized slender-body theory is applied to the computation of aerodynamic forces on an oscillating, or deforming, body in supersonic flow. The undeformed body is a body of revolution and the deformed body is represented by movement of a line through the centers of the cross sections which are assumed to remain circular. The time dependence is based on sinusoidal motion.

For a body of vanishing thickness the slender-body theory yields the apparent mass approximation as it is obtained for incompressible crossflow around a cylinder.

Both linearized slender-body theory and the apparent mass approximation are used to calculate the pitching-moment coefficients on a rigid slender body with a parabolic arc nose cone, and these coefficients are compared with some experimental results.

INTRODUCTION

The problem of predicting the dynamics of launch vehicles requires knowledge of the aerodynamic forces on an oscillating and/or a deforming body in high-speed flight. These forces are needed as an input to both the dynamic stability problem and as an input into the aero-servo-elastic problem. Especially important is the part of the ascent where the velocity is high and the atmospheric density is still great enough to cause significant aerodynamic reactions. The present analysis is concerned with this region which is generally the low supersonic part of the flight. This problem is considered in chapter 12 of reference 1 where references are given to other work. None of the references consulted have shown the type of slender-body approximation used here.

The analysis is by the linearized slender-body theory that has been widely used for steady flow phenomena. Although its reliability is limited to smooth slender bodies, it is the most accessible approach to the problem that is already complicated by the necessity for considering time dependence.

The motion of the body is defined as the deviation from a figure of revolution originally parallel to the line of flight. Both rigid movement and deformation are represented by lateral translation of the circular cross sections expressed in terms of the corresponding translation of a deforming center line.

The analysis is best suited for application to a pointed body. It can be formally applied to a blunt body but the approximate solution obtained is not usable near the nose. The type of shock wave formed by a blunt nose will alter the flow over the body and will affect the aerodynamic response to lateral motion.

The solution is obtained in a definite integral that has not been found to be integrable in finite form. Evaluation of the integral has been accomplished by numerical methods.

When the body radius is assumed to be vanishingly small, the solution degenerates to the well-known apparent mass approximation (ref. 2) that is obtained by regarding any cross section as a section from a two-dimensional incompressible flow. This approximation has the special feature that the aerodynamic force on any cross section depends only on the cross section and downwash, and their derivatives at that section.

NOTATION

a	speed of sound
b	center of rotation for rigid body motion
$\bar{c}$	diameter of base
C_m	pitching-moment coefficient, $\frac{\text{pitching moment}}{q_\infty S\bar{c}}$
I	moment of inertia of equivalent air mass
k	reduced frequency, $\frac{\omega l}{a}$
l	length of body
ΔL	local lift
ΔL_R	real part of $e^{-i\omega t}\Delta L$
ΔL_I	imaginary part of $e^{-i\omega t}\Delta L$
M	Mach number

q	angular velocity due to pitching
q_∞	free-stream dynamic pressure, $\frac{1}{2}\rho V^2$
(r,θ,x)	cylindrical space coordinates
R	radius of body
Re	real part
S	area of base
t	time
v	volume of body
V	free-stream velocity
W	downwash
$\overline{W}$	transformed downwash
W_o	amplitude of sinusoidal downwash
Z	displacement of center line
α	angle of attack
β	$\sqrt{M^2-1}$
ρ	air density
φ	velocity potential
$\overline{\varphi}$	transformed velocity potential
ψ	$\frac{\varphi}{\sin\theta}$
ω	circular frequency

When α, $\dot{\alpha}$, and q are used as subscripts, a dimensionless derivative is indicated.

$$C_{m_\alpha} = \left(\frac{\partial C_m}{\partial \alpha}\right) , \qquad C_{m_{\dot{\alpha}}} + C_{m_q} = \left[\frac{\partial C_m}{\partial(\dot{\alpha}\bar{c}/V)} + \frac{\partial C_m}{\partial(q\bar{c}/V)}\right]$$

A dot above a symbol denotes a derivative with respect to time.

STATEMENT OF THE PROBLEM

The linearized differential equation of the velocity potential φ for time dependent supersonic flow is, in cylindrical coordinates,

$$-\beta^2\varphi_{xx} + \varphi_{rr} + \frac{1}{r}\varphi_r + \frac{1}{r^2}\varphi_{\theta\theta} - \frac{2V}{a^2}\varphi_{xt} - \frac{1}{a^2}\varphi_{tt} = 0 \qquad (1)$$

The coordinates are fixed in space and the undisturbed flow ahead of the body is of velocity V in the direction of the positive x axis. The derivation of this equation and a discussion of its limitations are given in chapter I of reference 1. The form given here is equation A_2 of table I of that chapter, transformed to cylindrical coordinates. The axial distance downstream from the nose is given by x, and r and θ are polar coordinates in any plane of constant x (see sketch (a)). The radius of the cross section is $R(x)$ and the displacement of the line through the centers of the cross sections is $Z(x,t)$ in the direction $\theta = \pi/2$.

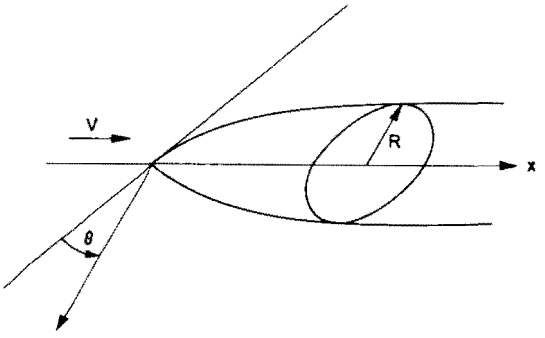

Sketch (a)

Then in the linearized approximation the boundary conditions for the part of φ that produces lift are

$$[\varphi_r]_{r=R(x)} = W(x,t) \sin\theta \qquad (2)$$

$$\varphi \to 0 \text{ as } r \to \infty \qquad (3)$$

where

$$W = Z_t + VZ_x \qquad (4)$$

The displacement of the center line $Z(x,t)$ can represent any plane translation, rotation, or deformation of the body. The variable $W(x,t)$ can be regarded as a form of downwash function if $\theta = \pi/2$ is directed downward. The solution satisfying boundary condition (2) in the slender-body approximation is dependent only on the function $R^2(x)W(x,t)$ for any W obtained by equation (4).

The local pressure change on the body is given by

$$\Delta p = -\rho[\varphi_t + V\varphi_x] + \cdots \qquad (5)$$

and the local lift per unit length is

$$\Delta L = \int_0^{2\pi} R\,\Delta p \sin\theta\, d\theta \qquad (6)$$

This lift ΔL is positive upward when Z and W are defined positive downward.

Quadratic terms that are sometimes important in Δp do not contribute to ΔL. Also, the axially symmetric disturbance velocity component of the flow does not produce lift and need not be considered.

ANALYSIS

The solution of equation (1) with boundary conditions (2) and (3) is obtained in appendix A. The surface boundary condition is applied through the usual slender-body approximation yielding a distribution of sources on the center line. The source strength at any point depends only on the body radius and motion at that cross section.

The method of solution is based on the use of Laplace transformations in t and x. The time transforms of φ and W are given in equations (A1) and (A2) of the appendix. The solution is obtained from the time transforms for the transform of ΔL in equation (A18) and the Laplace inversion for ΔL is given in equation (A19). This is a general result for any distributions of body cross section and center-line motion allowable in the slender-body approximation.

A simplified formulation is obtained if the time dependence is sinusoidal as defined in equation (A20). Then a steady sinusoidal solution for ΔL is obtained by equations (A17) and (A21). This is the form used in the subsequent calculations for the results of the slender-body theory.

A further simplification is obtained by the known apparent mass approximation that is formed here as a limit form for small body radius as stated in equation (A22). This approximation is used for comparison to the results of the more exact slender-body theory.

In the computations only sinusoidal time dependence will be considered, that is $W(x,t) = W_o(x)e^{i\omega t}$.

We assume that $W_o(x)R^2(x)$ is continuous over the length of the body. Since, in general, $W_o(x)R^2(x)$ cannot be represented by the same expression over the entire length of the body (e.g., parabolic arc nose and cylindrical body), we divide the body into k sections such that for each $x_j \leq x \leq x_{j+1}$

$$W_o(x)R^2(x) = W_j(x)R_j^2(x)$$

Then ΔL is given by equation (B7) in appendix B which is a derivation of the computation forms. Equation (B7) is sufficiently general

to cover a wide range of bodies and downwashes. However, we note that unless the first derivative of $W_o(x)R^2(x)$ is continuous at $x=x_j$, a singularity occurs at $x=x_j + \beta r$. This is where the Mach cone originating at $x=x_j$, $r=0$ intersects the surface of the body. Physically, there is no reason for such singularities. Mathematically, they exist because, while the problem prescribes boundary conditions on the surface of the body, the slender-body approximation gives a solution for an infinitely thin body, that is, the boundary conditions on the axis. Hence, linearized slender-body theory as used here breaks down locally for these cases. The problem can be circumvented by approximating the corners by polynomial curves in such a manner that $(d/dx)W_o(x)R^2(x)$ is continuous along the entire length of the body. This procedure is unnecessary unless some desired x falls very close to $x=x_j + \beta r$. Even with the above modification we do not know whether reasonable agreement with experiment would result for bodies with discontinuities. The best results from slender-body theory are expected for smooth bodies.

The computation forms have been programed for the IBM 704 for cases where $W_j(x)R_j^2(x)$ can be expressed as a polynomial of degree ≤ 9, and $J \leq 7$. Thus the program can be used directly for certain deforming bodies and is not confined to rigid body motions. The program also includes a numerical integration of the local lift to obtain the generalized forces defined by

$$F_q = \int_o^l \Delta L q(x)\,dx \tag{7}$$

where $q(x)$ is a polynomial in x, and l is the total length of the body. The machine computing run time varies from four minutes for a simple case where $J=1$ and 20 values of x are calculated to 30 minutes for a more complicated body with $J=7$ and x calculated for 52 values.

RIGID BODY MOTIONS

Both linearized theory and apparent mass theory were applied in the calculations of the forces on a simple body in rigid motion. Rigid body motions were chosen for the comparison because they were the simplest to compute and because experimental data can be obtained to check the theories much more readily than for flexible models. Rigid body oscillations should be sufficient to indicate theoretical accuracy. Moreover, the results are directly usable in the dynamic stability problem of the rigid missile.

For the case of a body of revolution pivoting about a point b, see sketch (b), we have

$$W_j(x)e^{i\omega t} = \alpha_o e^{i\omega t}[i\omega(x-b) + V] \tag{8}$$

We divide ΔL into its real and imaginary parts:

$$\Delta L = (\Delta L_R + i\Delta L_I)e^{i\omega t} \qquad (9)$$

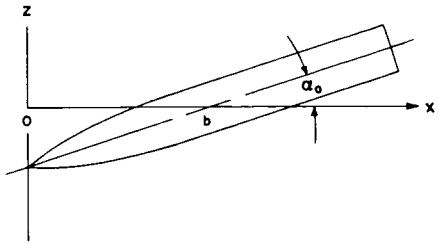

Sketch (b)

Then the equations of the dimensionless coefficients C_{m_α} and $C_{m_{\dot\alpha}} + C_{m_q}$ are:

$$C_{m_\alpha} = \frac{1}{q_\infty S\bar{c}\alpha_o}\int_o^l \Delta L_R(b-x)\,dx \qquad (10)$$

$$C_{m_{\dot\alpha}} + C_{m_q} = \frac{V}{q_\infty S\bar{c}^2\omega\alpha_o}\int_o^l \Delta L_I(b-x)\,dx \qquad (11)$$

where

S area of the base

$\bar{c}$ diameter of the base

If equation (B7) is used in equations (10) and (11), the integrations must be done numerically since ΔL_R and ΔL_I cannot be integrated analytically. However, the machine program permits the choice of as many values of x as desired for ΔL.

The apparent mass formulas for C_{m_α} and $C_{m_{\dot\alpha}} + C_{m_q}$ may be written:

$$C_{m_\alpha} = \frac{2v}{S\bar{c}} - \frac{2}{\bar{c}}(l-b) + \frac{\omega^2 I}{q_\infty S\bar{c}} \qquad (12)$$

v volume of the body

I moment of inertia of an equivalent air mass referred to the center of rotation

$$C_{m_{\dot\alpha}} + C_{m_q} = \frac{-2}{\bar{c}^2}(l-b)^2 \quad \text{(ref. 3)} \qquad (13)$$

Note that $C_{m_{\dot\alpha}} + C_{m_q}$ is independent of Mach number and frequency.

COMPARISON AND DISCUSSION

The coefficients C_{m_α} and $C_{m_{\dot{\alpha}}} + C_{m_q}$ were calculated for a body with parabolic arc nose and fineness ratio 10 (see sketch (b)). The equations for the radius are:

$$R(x)_{in} = \frac{x}{90}(30-x) \qquad 0 \leq x \leq 15 \text{ in.}$$

$$R(x)_{in} = 2.5 \qquad 15 \leq x \leq 50 \text{ in.}$$

Both the linearized theory and apparent mass formulas were used. Also, wind-tunnel tests were run on such a body in the Ames 14-Foot Transonic and Unitary Plan Wind Tunnels. Figures 1 and 2 show the results for C_{m_α} and $C_{m_{\dot{\alpha}}} + C_{m_q}$ plotted against the center of rotation for Mach numbers 1.1 and 1.2. At Mach number 1.1 and frequency 10 cps $(k=5\pi/72)$, both theories agreed well with experiment. The agreement at $M=1.2$ was less satisfactory. At low Mach numbers and frequencies there seems to be little reason for using the slender-body theory solutions instead of the simpler apparent mass ones, at least in the case of rigid body motions. Figures 3 and 4 show the effect of increasing Mach number on the theoretical values of C_{m_α} and $C_{m_{\dot{\alpha}}} + C_{m_q}$. Both slender-body and experimental results show increase in coefficients with increasing Mach number, but the apparent mass results show little change. Therefore, it appears that for the higher Mach numbers, slender-body theory solutions are superior to those derived from apparent mass. Figures 5 and 6 show the ratio of results of the slender-body theory to those for the apparent mass as Mach number increases. In figure 5 the curves for $b/l = 0.4$ and 0.6 practically coincided with $b/l = 0.5$; hence they are not included. Figures 7 and 8 show the effect in increasing frequencies on theoretical values of C_{m_α} and $C_{m_{\dot{\alpha}}} + C_{m_q}$. The effect of frequency is about the same for both theories. The difference in the absolute values is primarily a Mach number effect. Figures 9 and 10 compare the local lift as computed by slender-body theory and apparent mass theory at $M=1.2$ and $M=2$. A significant increase in the difference in the lift distribution at the higher Mach number is noted.

CONCLUDING REMARKS

For low supersonic Mach number and low frequency oscillation, the linearized slender-body theory used here has no advantage over the conventional apparent mass approximation using the mass of displaced air.

For higher Mach numbers the theory shows the local lift and, in general, the integrated lift and moment, to be larger than those obtained by the apparent mass approximation. This increase has also been found experimentally.

For higher frequency of oscillation the theory indicates an increase over the apparent mass result but this does not appear likely to be large for frequencies that might be encountered. No experimental results have been obtained for the effect of frequency.

The slender-body theory is limited to smooth pointed bodies. Rapid but continuous changes of cross section even with continuous slope cause uncertainties in the results.

Ames Research Center
National Aeronautics and Space Administration
Moffett Field, Calif., Feb. 28, 1961

APPENDIX A

SOLUTION OF THE LINEARIZED SLENDER-BODY EQUATIONS WITH TIME DEPENDENCE

The differential equation (1)

$$-\beta^2\varphi_{xx} + \varphi_{rr} + \frac{1}{r}\varphi_r + \frac{1}{r^2}\varphi_{\theta\theta} - \frac{2V}{a^2}\varphi_{xt} - \frac{1}{a^2}\varphi_{tt} = 0 \tag{1}$$

is to be solved for the boundary conditions (2) and (3)

$$[\varphi_r]_{r=R(x)} = W(x,t)\sin\theta \tag{2}$$

$$\varphi \to 0 \text{ as } r \to \infty \tag{3}$$

The use of Laplace transforms provides a convenient method of solution. Time transforms of φ and W are taken in the form

$$\bar{\varphi} = \int_0^\infty e^{-st}\varphi \, dt \tag{A1}$$

$$\bar{W} = \int_0^\infty e^{-st}W \, dt, \qquad \mathrm{Re}(s) > 0 \tag{A2}$$

The remaining variables are unaffected by this transformation and equation (1) becomes

$$-\beta^2\bar{\varphi}_{xx} + \bar{\varphi}_{rr} + \frac{1}{r}\bar{\varphi}_r + \frac{1}{r^2}\bar{\varphi}_{\theta\theta} - \frac{2Vs}{a^2}\bar{\varphi}_x - \frac{s^2}{a^2}\bar{\varphi} = 0 \tag{A3}$$

The boundary conditions (2) and (3) become

$$[\bar{\varphi}_r]_{r=R(x)} = \bar{W}\sin\theta \tag{A4}$$

$$\bar{\varphi} \to 0 \text{ as } r \to \infty \tag{A5}$$

The transformations take this form when φ and W vanish for $t \leq 0$.

The only solution of equation (1) compatible with boundary conditions (2) is of the form

$$\varphi(x,r,\theta,t) = \psi(x,r,t)\sin\theta \tag{A6}$$

and after transformation (A1)

$$\bar{\Phi}(x,r,\theta) = \bar{\Psi}(x,r)\sin\theta \tag{A7}$$

The differential equation and boundary conditions now become

$$-\beta^2\bar{\Psi}_{xx} + \bar{\Psi}_{rr} + \frac{1}{r}\bar{\Psi}_r - \frac{1}{r^2}\bar{\Psi} - \frac{2Vs}{a^2}\bar{\Psi}_x - \frac{s^2}{a^2}\bar{\Psi} = 0 \tag{A8}$$

and

$$[\bar{\Psi}_r]_{r=R(x)} = \bar{W}(x) \tag{A9}$$

$$\bar{\Psi} \to 0 \text{ as } r \to \infty \tag{A10}$$

Separation of variables in equation (A8) yields a solution in the form

$$e^{\lambda x}K_1(\sigma r) \tag{A11}$$

where K_1 is the first order modified Bessel function of the second kind and

$$\sigma = \sqrt{\beta^2\lambda^2 + \frac{2Vs\lambda}{a^2} + \frac{s^2}{a^2}}$$

with

$$\mathrm{Re}(\sigma) > 0 \text{ for } \mathrm{Re}(\lambda) > 0 \text{ and } \mathrm{Re}(s) > 0$$

The selection of the K_1 solution of the modified Bessel equation is necessary to satisfy boundary condition (A10).

The solution of equation (A9) is sought as an integral of solutions in the form of an inverse Laplace transform

$$\bar{\Psi}(x,r) = \frac{1}{2\pi i}\int_{c-i\infty}^{c+i\infty} e^{\lambda x}K_1(\sigma r)f(\lambda)d\lambda \ , \qquad c > 0 \tag{A12}$$

At this point the slender-body approximation is introduced by replacing K_1 by its approximate value for small r

$$K_1(\sigma r) \approx \frac{1}{\sigma r} \tag{A13}$$

and, to this approximation

$$\bar{\psi}(x,r) = \frac{1}{2\pi i}\int_{c-i\infty}^{c+i\infty} e^{\lambda x}\,\frac{1}{\sigma r}\,f(\lambda)\,d\lambda$$

Differentiating and substituting in equation (A9)

$$\bar{W}(x) = \frac{1}{2\pi i}\int_{c-i\infty}^{c+i\infty} e^{\lambda x}\,\frac{1}{\sigma R^2(x)}\,f(\lambda)\,d\lambda$$

or, rearranging

$$\frac{1}{2\pi i}\int_{c-i\infty}^{c+i\infty} \frac{e^{\lambda x} f(\lambda)}{\sigma}\,d\lambda = -R^2(x)\bar{W}(x)$$

and by the Laplace inversion formula

$$\frac{f(\lambda)}{\sigma} = -\int_0^\infty e^{-\lambda x'} R^2(x')\bar{W}(x')\,dx'$$

Putting this in equation (A12)

$$\bar{\psi}(x,r) = -\frac{1}{2\pi i}\int_{c-i\infty}^{c+i\infty} e^{\lambda x} K_1(\sigma r)\sigma\,d\lambda \int_0^\infty e^{-\lambda x'} R^2(x')\bar{W}(x')\,dx' \qquad (A14)$$

This is a repeated integral that does not permit reversal of the order of integration. It can be put in a form that does permit the reversal by expression as a derivative.

$$\bar{\psi}(x,r) = \frac{\partial}{\partial r}\,\frac{1}{2\pi i}\int_{c-i\infty}^{c+i\infty} e^{\lambda x} K_0(\sigma r)\,d\lambda \int_0^\infty e^{-\lambda x'} R^2(x')\bar{W}(x')\,dx'$$

$$= \frac{\partial}{\partial r}\int_0^\infty R^2(x')\bar{W}(x')\,dx' \left[\frac{1}{2\pi i}\int_{c-i\infty}^{c+i\infty} e^{\lambda(x-x')} K_0(\sigma r)\,d\lambda\right] \qquad (A15)$$

The integral in the brackets in equation (A15) can be reduced to a standard form by the substitution

$$\zeta = \lambda + \frac{Vs}{\beta^2 a^2}$$

and it becomes

$$e^{-\frac{Vs}{\beta^2 a^2}(x-x')} \frac{1}{2\pi i}\int_{c_1-i\infty}^{c_1+i\infty} e^{\zeta(x-x')} K_o\left[\beta r\sqrt{\zeta^2-\left(\frac{s}{\beta^2 a}\right)^2}\right]d\zeta$$

with

$$c_1 > \frac{s}{\beta^2 a}$$

The integral is obtainable from (47), page 284, reference 4, and is reducible to elementary form by noting that

$$I_{-1/2}(x) = \sqrt{\frac{2}{\pi x}}\cosh x$$

Then, observing the reduced limit on the x' integration in (A15)

$$\bar{\psi}(x,r) = \frac{\partial}{\partial r}\int_o^{x-\beta r} \frac{e^{-\frac{Ms}{\beta^2 a}(x-x')}\cosh\left[\frac{s}{\beta^2 a}\sqrt{(x-x')^2-\beta^2 r^2}\right]}{\sqrt{(x-x')^2-\beta^2 r^2}} R^2(x')\bar{W}(x')dx' \tag{A16}$$

From equations (2) and (5)

$$\Delta L = -\rho\int_o^{2\pi} R[\varphi_t + V\varphi_x]\sin\theta\, d\theta$$

and from equations (6) and (A6)

$$\Delta L = -\rho\int_o^{2\pi} R[\psi_t + V\psi_x]\sin^2\theta\, d\theta$$

$$= -\pi\rho R[\psi_t + V\psi_x] \tag{A17}$$

Then the time transform of ΔL is

$$\Delta\bar{L} = -\pi\rho R[s\bar{\psi} + V\bar{\psi}_x] \tag{A18}$$

For the general case, with Z = constant and therefore $W = 0$ for $t \leq 0$, the transform $\bar{W}$ is obtained by equation (A2) and then $\bar{\psi}$ is formed by the integration in equation (A16). Then after substitution in equation (A18) an inverse Laplace transformation yields

$$\Delta L = \frac{1}{2\pi i}\int_{c-i\infty}^{c+i\infty} e^{st}\Delta\bar{L}\, ds \quad , \qquad c > 0 \tag{A19}$$

For a sinusoidal motion of the form described by

$$\left.\begin{aligned} Z(x,t) &= Z_o(x)e^{i\omega t} \\ W(x,t) &= W_o(x)e^{i\omega t} \end{aligned}\right\} \tag{A20}$$

it is possible to obtain a steady oscillatory solution. In this case

$$\bar{W}(x) = \frac{W_o(x)}{s-i\omega}$$

and using equation (A16) in the Laplace inversion

$$\psi = \frac{1}{2\pi i}\int_{c-i\infty}^{c+i\infty} e^{st}\bar{\psi}\, ds$$

and reversing the order of integration

$$\psi = \frac{\partial}{\partial r}\int_o^{x-\beta r} \frac{R^2(x')W_o(x')}{\sqrt{(x-x')^2-\beta^2r^2}}\, dx' \; \frac{1}{2\pi i}\int_{c-i\infty}^{c+i\infty} e^{s\left[t - \frac{M}{\beta^2 a}(x-x')\right]} \cosh\left[\frac{s}{\beta^2 a}\sqrt{(x-x')^2-\beta^2r^2}\right]\frac{ds}{s-i\omega}$$

For $t > x/V-a$ the oscillation of ψ is steady and the inner integral is given by the residue at $s=i\omega$ and

$$\psi = e^{i\omega t}\frac{\partial}{\partial r}\int_o^{x-\beta r} \frac{e^{-\frac{i\omega M}{\beta^2 a}(x-x')}\cos\left[\frac{\omega}{\beta^2 a}\sqrt{(x-x')^2-\beta^2r^2}\right]}{\sqrt{(x-x')^2-\beta^2r^2}} R^2(x')W_o(x')dx' \tag{A21}$$

From this result ΔL is formed by substitution in equation (A17).

The above results were obtained by the usual slender-body approximation. The same approximation can be used to obtain a simplified result from equation (A14). If the approximation (A13) is introduced, equation (A14) becomes

$$\bar{\psi} = -\frac{1}{r}\frac{1}{2\pi i}\int_{c-i\infty}^{c+i\infty} e^{\lambda x} d\lambda \int_{0}^{\infty} e^{-\lambda x'} R^2(x')\bar{W}(x')dx'$$

$$= -\frac{1}{r} R^2(x)\bar{W}(x) \qquad \text{for} \quad x > 0$$

from the Laplace transformation and its immediate inversion. A time inversion of $\bar{\psi}$ and $\bar{W}$ yields

$$\psi = -\frac{1}{r} R^2(x)W(x,t)$$

and

$$\Delta L = \pi\rho\left(\frac{\partial}{\partial t} + V\frac{\partial}{\partial x}\right)\left[R^2(x)W(x,t)\right] \tag{A22}$$

This is the usual time dependent generalization of the apparent mass concept as used by Munk (ref. 2). It should be noted that ΔL of equation (A22) depends on R and W and their derivatives at the point x at time t and is not affected by the shape of the remainder of the body or by any events at earlier time.

APPENDIX B

DERIVATION OF COMPUTATION FORMS FOR LINEARIZED SLENDER-BODY THEORY

From equations (A17) and (A21) we have

$$\Delta L = \pi\rho R[\psi_t + V\psi_x] \tag{A17}$$

$$\psi = e^{i\omega t}\frac{\partial}{\partial r}\int_o^{x-\beta r}\frac{e^{-\frac{i\omega M}{\beta^2 a}(x-x')}\cos\left[\frac{\omega}{\beta^2 a}\sqrt{(x-x')^2-\beta^2r^2}\right]}{\sqrt{(x-x')^2-\beta^2r^2}}R^2(x')W_o(x')dx' \tag{A21}$$

where ψ and ψ_x are evaluated at $r=R(x)$.

Dividing the body into k sections by planes perpendicular to the axis so that for each $x_j \le x \le x_{j+1}$

$$W_o(x)R^2(x) = W_j(x)R_j^2(x)$$

we have

$$\left.\begin{aligned}\psi = e^{i\omega t}\frac{\partial}{\partial r}\sum_{j=o}^{J}\int_{x_j}^{x_{j+1}} e^{-\frac{i\omega M}{\beta^2}(x-x')}\cos\left[\frac{\omega}{\beta^2 a}\sqrt{(x-x')^2-\beta^2r^2}\right]\frac{W_j(x')R_j^2(x')dx'}{\sqrt{(x-x')^2-\beta^2r^2}}\\ x_o \equiv 0\\ x_{J+1} \equiv x-\beta r\end{aligned}\right\} \tag{B1}$$

To carry the differentiation under the integral sign, we make the substitution:

$$(x-x') = \beta r \sec\theta \tag{B2}$$

Applying (B2) and carrying out the indicated differentiation gives:

$$\psi = \frac{e^{i\omega t}}{r}\left\{ -\sum_{j=o}^{J} \frac{(x-x_j)e^{-\frac{i\omega M}{\beta^2 a}(x-x_j)}}{\sqrt{(x-x_j)^2-\beta^2r^2}} \cos\left[\frac{\omega}{\beta^2 a}\sqrt{(x-x_j)^2-\beta^2r^2}\right] W_j(x_j)R_j^2(x_j) \right.$$

$$+\sum_{j=o}^{J-1} \frac{(x-x_{j+1})e^{-\frac{i\omega M}{\beta^2 a}(x-x_{j+1})}}{\sqrt{(x-x_{j+1})^2-\beta^2r^2}} \cos\left[\frac{\omega}{\beta^2 a}\sqrt{(x-x_{j+1})^2-\beta^2r^2}\right] W_j(x_{j+1})R_j^2(x_{j+1})$$

$$-\sum_{j=o}^{J} r\int_{\arccos\left(\frac{\beta r}{x-x_{j+1}}\right)}^{\arccos\left(\frac{\beta r}{x-x_j}\right)} e^{-\frac{i\omega M}{\beta^2 a}\beta r \sec\theta}\left[\frac{i\omega M}{\beta a}\sec^2\theta \cos\left(\frac{\omega}{\beta^2 a}\beta r\tan\theta\right) W_j(x-\beta r\sec\theta)R_j^2(x-\beta r\sec\theta)\right.$$

$$+\frac{\omega}{\beta a}\sec\theta\tan\theta \sin\left(\frac{\omega}{\beta^2 a}\beta r\tan\theta\right) W_j(x-\beta r\sec\theta)R_j^2(x-\beta r\sec\theta)$$

$$\left.\left.+\beta\sec^2\theta \cos\left(\frac{\omega}{\beta^2 a}\beta r\tan\theta\right)\frac{\partial}{\partial x}W_j(x-\beta r\sec\theta)R_j^2(x-\beta r\sec\theta)\right]\right\} d\theta \qquad (B3)$$

If we assume that the $W_j(x)R_j(x)$ are continuous at the x_j, that is,

$$W_j(x_{j+1})R_j^2(x_{j+1}) = W_{j+1}(x_{j+1})R_{j+1}^2(x_{j+1}) \qquad (B4)$$

and that $R(0) = 0$, the constant term vanishes.

$$\psi = -e^{i\omega t}\sum_{j=o}^{J}\int_{\arccos\left(\frac{\beta r}{x-x_{j+1}}\right)}^{\arccos\left(\frac{\beta r}{x-x_j}\right)} e^{-\frac{i\omega M}{\beta^2 a}\beta r\sec\theta}\left[\frac{i\omega M}{\beta a}\sec\theta \cos\left(\frac{\omega}{\beta^2 a}\beta r\tan\theta\right) W_j(x-\beta r\sec\theta)R_j^2(x-\beta r\sec\theta)\right.$$

$$+\frac{\omega}{\beta a}\tan\theta \sin\left(\frac{\omega}{\beta^2 a}\beta r\tan\theta\right) W_j(x-\beta r\sec\theta)R_j^2(x-\beta r\sec\theta)$$

$$\left.+\beta\sec\theta \cos\left(\frac{\omega}{\beta^2 a}\beta r\tan\theta\right)\frac{\partial}{\partial x}W_j(x-\beta r\sec\theta)R_j^2(x-\beta r\sec\theta)\right]\sec\theta\, d\theta \qquad (B5)$$

From equation (A17)

$$\Delta L = -\pi\rho R[\psi_t + V\psi_x] \qquad (A17)$$

$$\psi_t = i\omega\psi \qquad (B6)$$

The calculation of ψ_x is straightforward. If we apply (B4) to the result and change the integration variable by the substitution

$$\xi = \beta r \tan \theta$$

Then, letting $r = R(x)$, we obtain the form

$$\Delta L = \pi \rho e^{i\omega t} \left(\frac{e^{-\frac{i\omega M x}{\beta^2 a}} 2Vx}{\sqrt{x^2-\beta^2 r^2}} \cos\left(\frac{\omega}{\beta^2 a}\sqrt{x^2-\beta^2 r^2}\right) W_o(0) R_o(0) \left[\frac{d}{dx'} R_o(x')\right]_{x'=0} \right.$$

$$+ \sum_{j=1}^{J} \frac{e^{-\frac{i\omega M}{\beta^2 a}(x-x_j)} V(x-x_j)}{\sqrt{(x-x_j)^2-\beta^2 r^2}} \cos\left[\frac{\omega}{\beta^2 a}\sqrt{(x-x_j)^2-\beta^2 r^2}\right] \frac{d}{dx'}\left[W_j(x') R_j^2(x') - W_{j-1}(x') R_{j-1}^2(x')\right]_{x'=x_j}$$

$$+ \sum_{j=o}^{J} \int_{\sqrt{(x-x_{j+1})^2-\beta^2 r^2}}^{\sqrt{(x-x_j)^2-\beta^2 r^2}} e^{-\frac{i\omega M}{\beta^2 a}(\xi^2+\beta^2 r^2)} \left\{ \left(-\frac{\omega^2 M}{\beta^2 a}\cos\frac{\omega\xi}{\beta^2 a} + \frac{i\omega^2 \xi}{\beta^2\sqrt{\xi^2+\beta^2 r^2}}\sin\frac{\omega\xi}{\beta^2 a}\right) W_j(x-\sqrt{\xi^2+\beta^2 r^2}) R_j^2(x-\sqrt{\xi^2+\beta^2 r^2}) \right.$$

$$+ \left[\frac{i\omega}{\beta^2}(M^2+\beta^2)\cos\frac{\omega\xi}{\beta^2 a} + \frac{\omega M\xi}{\beta^2\sqrt{\xi^2+\beta^2 r^2}}\sin\frac{\omega\xi}{\beta^2 a}\right] \frac{\partial}{\partial x} W_j(x-\sqrt{\xi^2+\beta^2 r^2}) R_j^2(x-\sqrt{\xi^2+\beta^2 r^2})$$

$$\left. \left. + V\cos\frac{\omega\xi}{\beta^2 a}\frac{\partial^2}{\partial x^2} W_j(x-\sqrt{\xi^2+\beta^2 r^2}) R_j^2(x-\sqrt{\xi^2+\beta^2 r^2}) \right\} d\xi \right) \qquad \text{(B7)}$$

For $[(d/dx)R_o(x)]_{x=o} < \infty$ (i.e., sharp-nosed bodies), the first term vanishes. If the slopes are continuous at the x_j as well as the downwash and its first x derivative, all the constant terms are zero.

APPENDIX C

DERIVATION OF C_{m_α} AND $C_{m_{\dot\alpha}} + C_{m_q}$ FROM APPARENT MASS THEORY

From equation (A8) we have

$$\Delta L = \pi\rho \left(\frac{\partial}{\partial t} + V \frac{\partial}{\partial x}\right) W(x,t) R^2(x) \tag{C1}$$

In the case of sinusoidal time dependent motion,

$$W(x,t) = W_o(x) e^{i\omega t} \tag{C2}$$

For rigid body motions

$$W(x,t) = (z_t + V z_x) \tag{C3}$$

where $z = \alpha_o(x-b)e^{i\omega t}$ and b is the center of rotation. Substituting in (C1)

$$\Delta L = \pi\rho\alpha_o \left(\frac{\partial}{\partial t} + V \frac{\partial}{\partial x}\right) [i\omega(x-b)+V] R^2(x) e^{i\omega t} \tag{C4}$$

$$\Delta L = \pi\rho e^{i\omega t}\alpha_o \left\{-\omega^2(x-b)R^2(x) + V^2 \frac{d}{dx} R^2(x) + i\omega V \left[\frac{d}{dx}(x-b)R^2(x) + R^2(x)\right]\right\} \tag{C5}$$

$$\Delta L_R = \alpha_o \pi\rho \left[-\omega^2(x-b)R^2(x) + V^2 \frac{d}{dx} R^2(x)\right] \tag{C5a}$$

$$\Delta L_I = \pi\rho\omega V\alpha_o \left[\frac{d}{dx}(x-b)R^2(x) + R^2(x)\right] \tag{C5b}$$

Substituting (C5a) into equation (10) and (C5b) into equation (11)

$$C_{m_\alpha} = \frac{2\pi}{S\bar{c}} \int_o^l \left[\frac{\omega^2}{\rho V^2} \rho(x-b)^2 R^2(x) + (b-x) \frac{d}{dx} R^2(x) dx\right] \tag{C6}$$

The first term equals $(\omega^2/q_o S\bar{c})I$ where I is the moment of inertia of an equivalent air mass with respect to the center of rotation. Integrating the second term by parts gives

$$\frac{2\pi}{S\bar{c}}(b-l)R^2(l) + \frac{2\pi}{S\bar{c}}\int_o^l R^2(x)dx$$

which equals $[-2(l-b)/\bar{c}]+[2v/S\bar{c}]$ where v is the volume of the body Therefore

$$C_{m_\alpha} = \frac{2v}{S\bar{c}} - \frac{2}{\bar{c}}(l-b) + \frac{\omega^2}{q_o S\bar{c}} I \qquad (C7)$$

The solution represented by (C7) was not found in any of the available references.

$$C_{m_{\dot{\alpha}}} + C_{m_q} = \frac{2\pi}{S\bar{c}^2}\int_o^l \left[(b-x)\frac{d}{dx}(x-b)R^2(x) + (b-x)R^2(x)\right]dx \qquad (C8)$$

Integrating the first term by parts and combining gives

$$-\frac{2\pi}{S\bar{c}^2}(l-b)^2R^2(l) + \frac{2\pi}{S\bar{c}^2}\int_o^l \left[(x-b)R^2(x) + (b-x)R^2(x)\right]dx \qquad (C9)$$

Therefore

$$C_{m_{\dot{\alpha}}} + C_{m_q} = \frac{-2(l-b)^2}{\bar{c}^2} \qquad (C10)$$

(Equation (C10) is derived by Tobak, et al., in ref. 3. This derivation is included here for completeness.)

REFERENCES

1. Miles, John W.: The Potential Theory of Unsteady Supersonic Flow. Cambridge University Press, 1959.

2. Munk, Max M.: The Aerodynamic Forces on Airship Hulls. NACA Rep. 184, 1924.

3. Tobak, Murray, Reese, David E., Jr., and Beam, Benjamin H.: Experimental Damping in Pitch of 45° Triangular Wings. NACA RM A50J26, 1950.

4. Erdélyi, A.: Tables of Integral Transforms, vol. 1. McGraw-Hill Book Co., Inc., 1954.

Page intentionally left blank

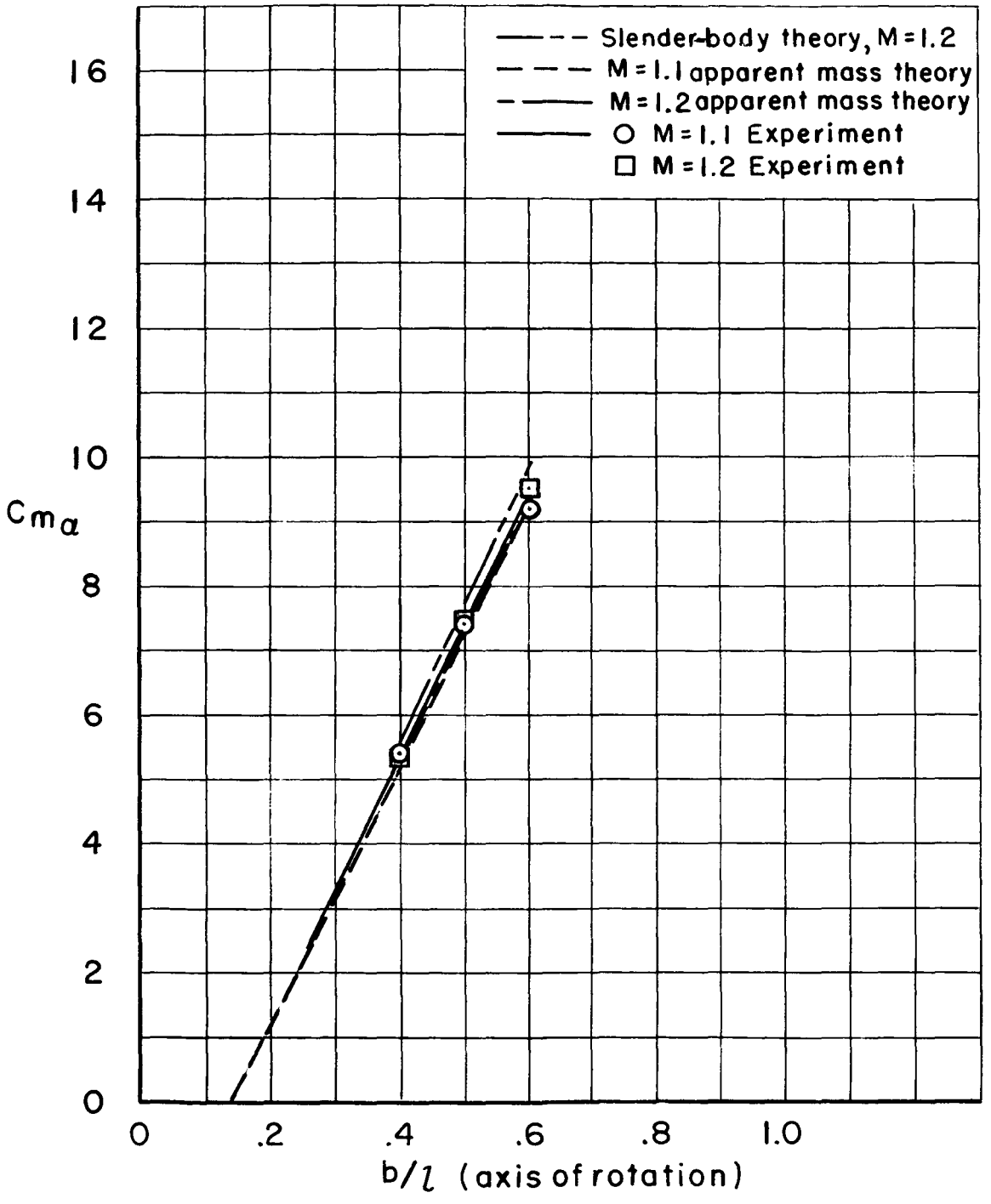

Figure 1.- Experimental and theoretical C_{m_α} for $\alpha = 0^\circ$, $k = 5\pi/72$ for slender body with parabolic arc nose cone.

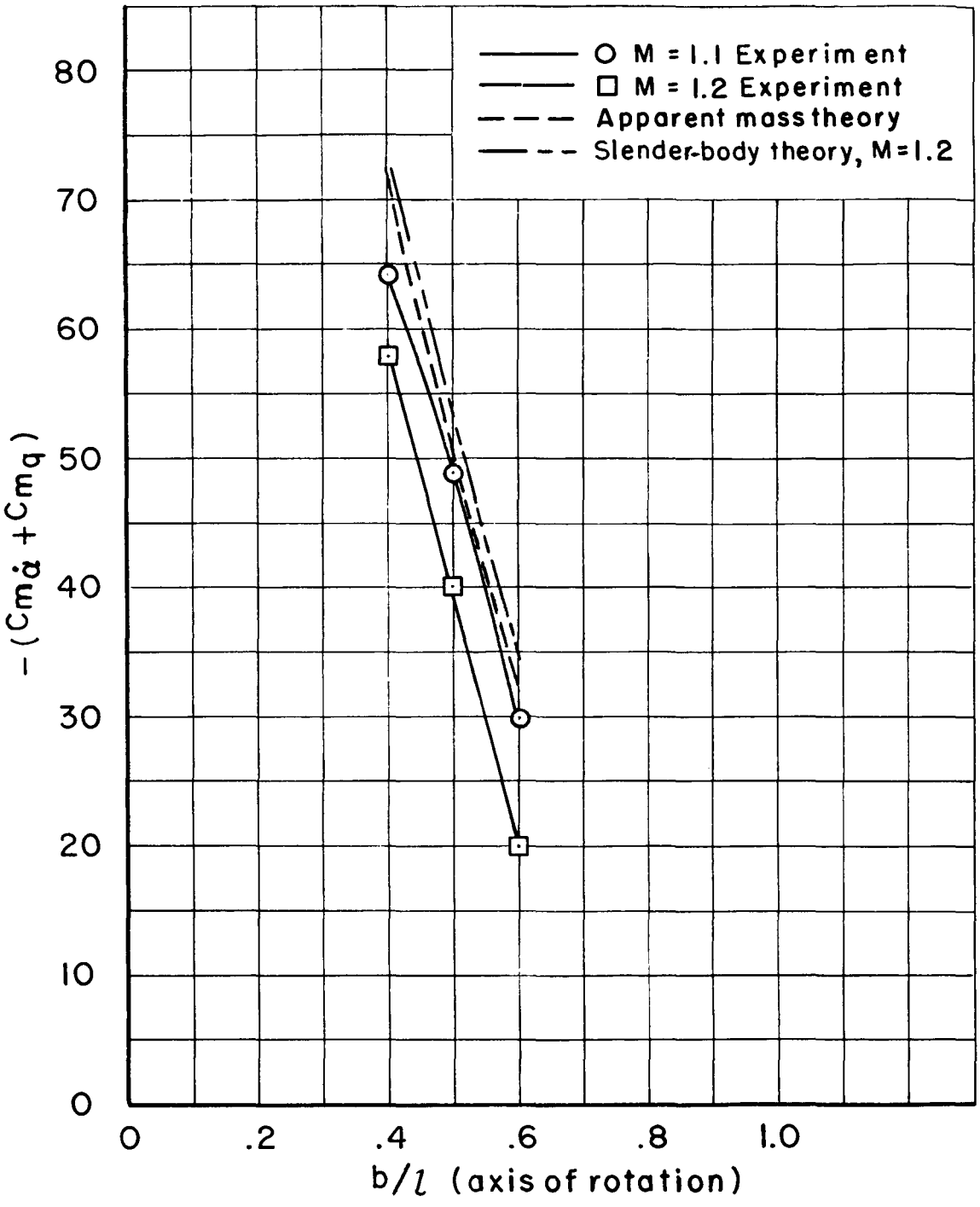

Figure 2.- Experimental and theoretical $C_{m_\alpha} + C_{m_q}$ for slender body with parabolic arc nose cone for $\alpha = 0^\circ$, $k = 5\pi/72$.

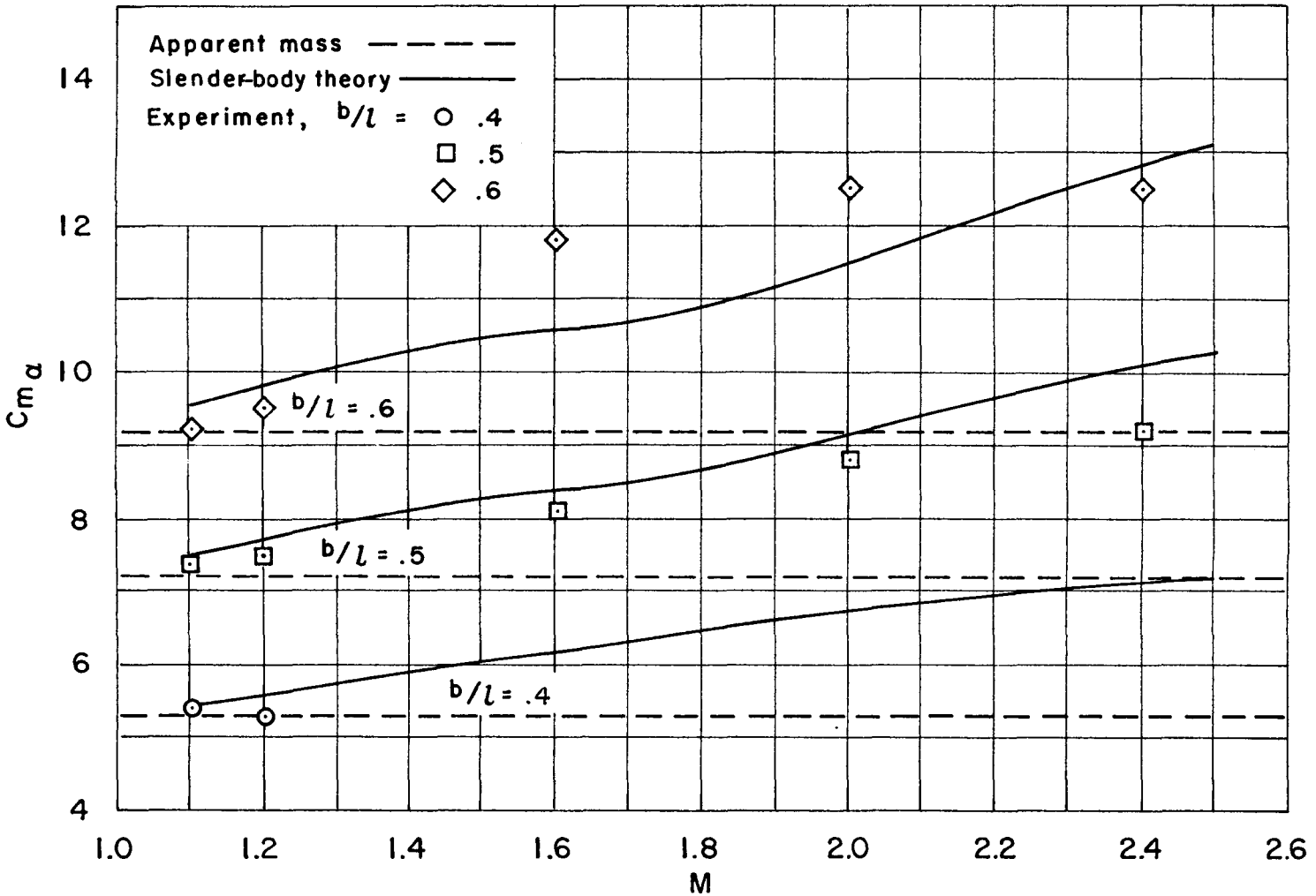

Parabolic arc nose cone
$\omega l/a = 5\pi/72$

Figure 3.- Effect of increasing Mach number on C_{m_α}.

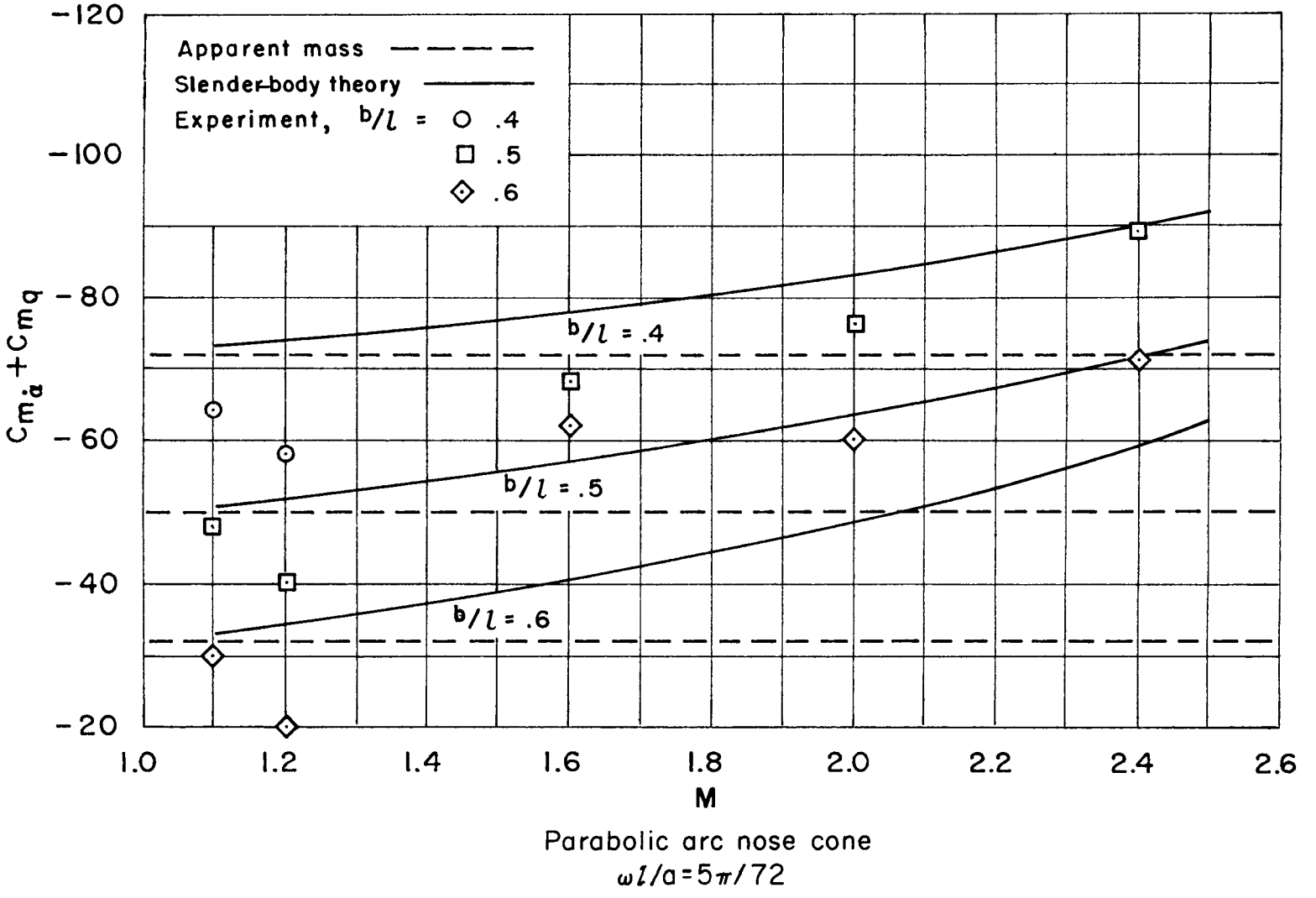

Figure 4.- Effect of increasing Mach number on $C_{m_{\dot{\alpha}}} + C_{m_q}$.

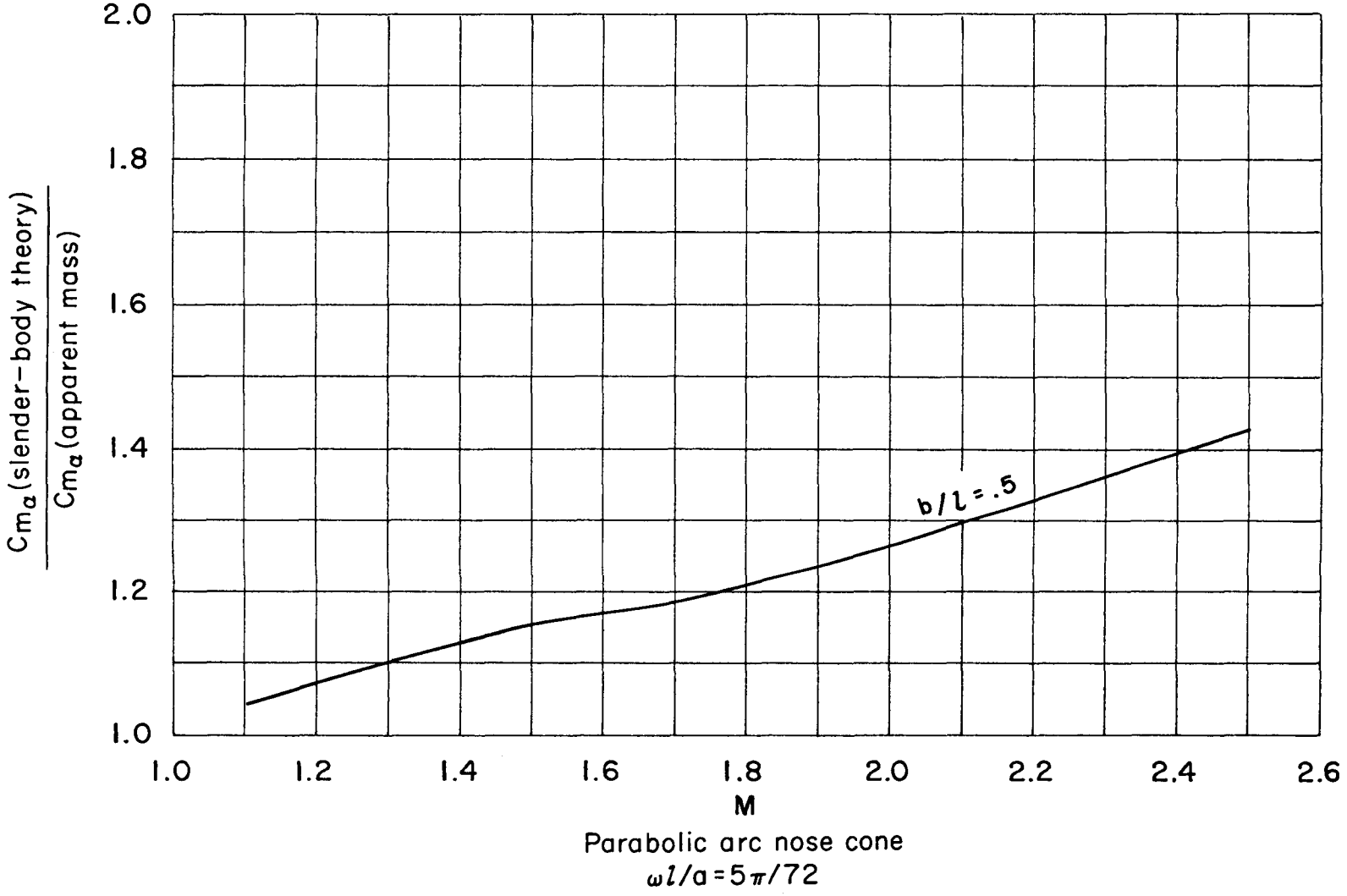

Figure 5.- Ratio of slender-body theory results to apparent mass theory results; C_{m_α}.

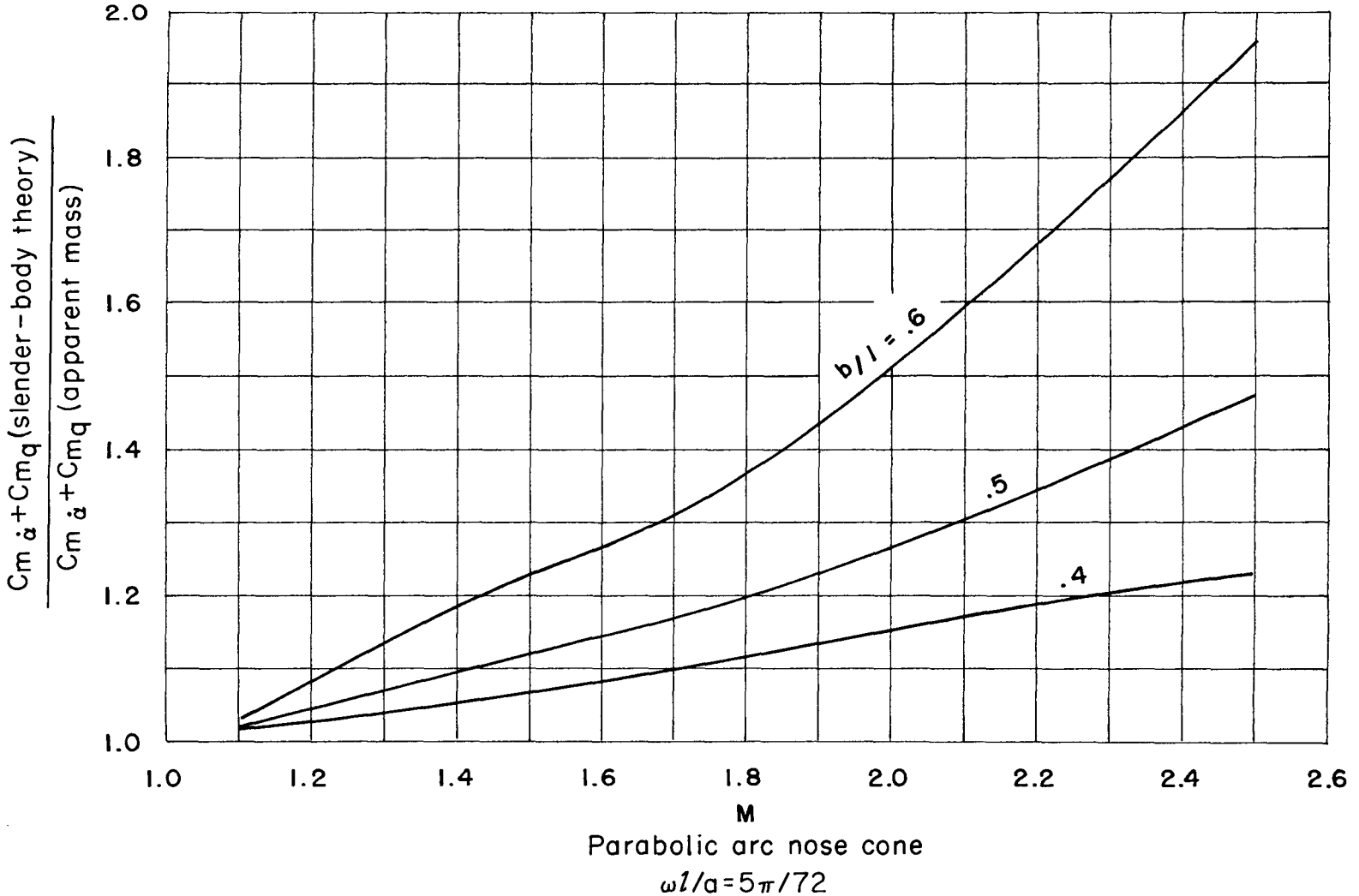

Figure 6.- Ratio of slender-body theory results to apparent mass theory results; $C_{m_{\dot{\alpha}}} + C_{m_q}$.

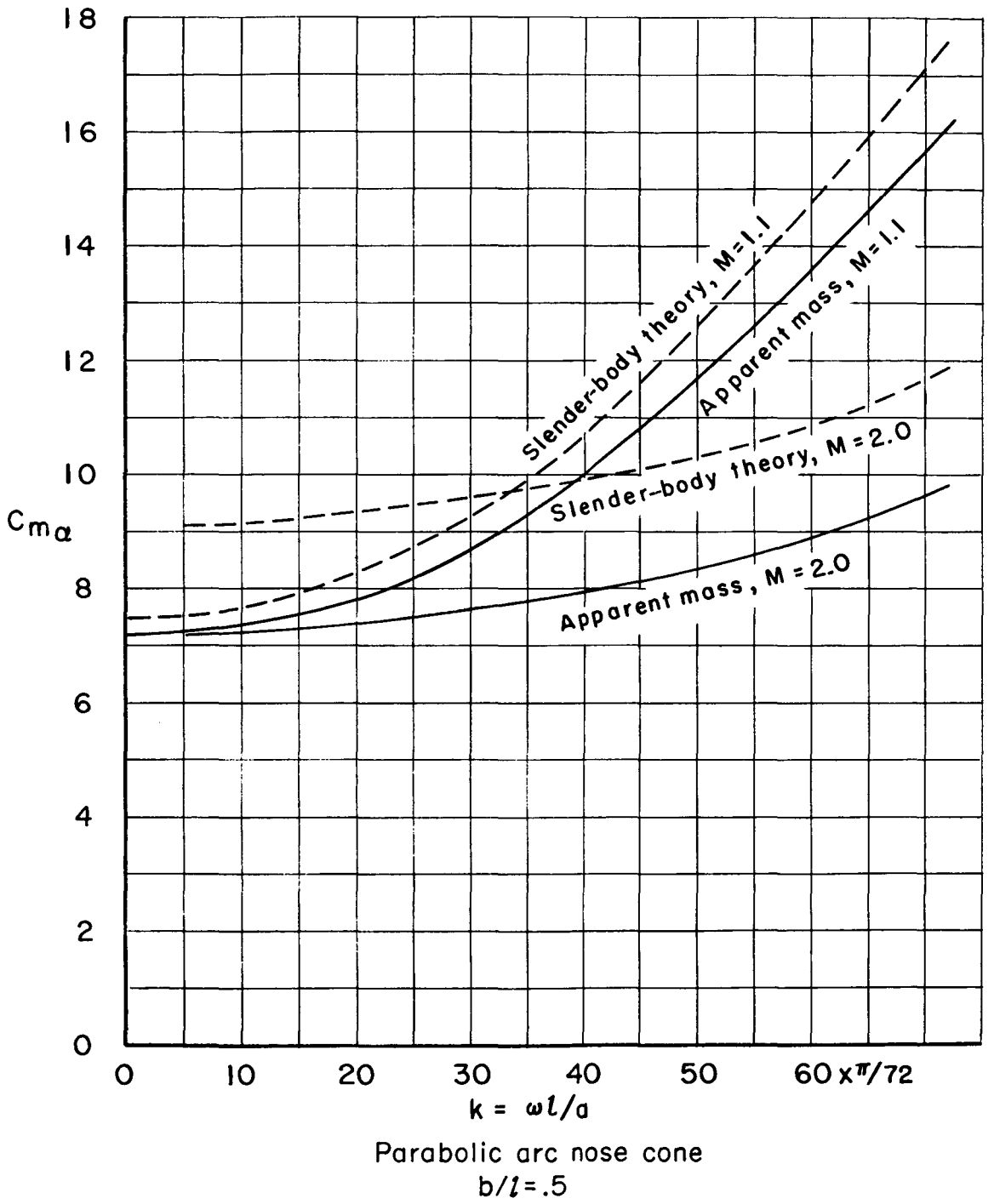

Figure 7.- Effect of increasing frequency on C_{m_α}.

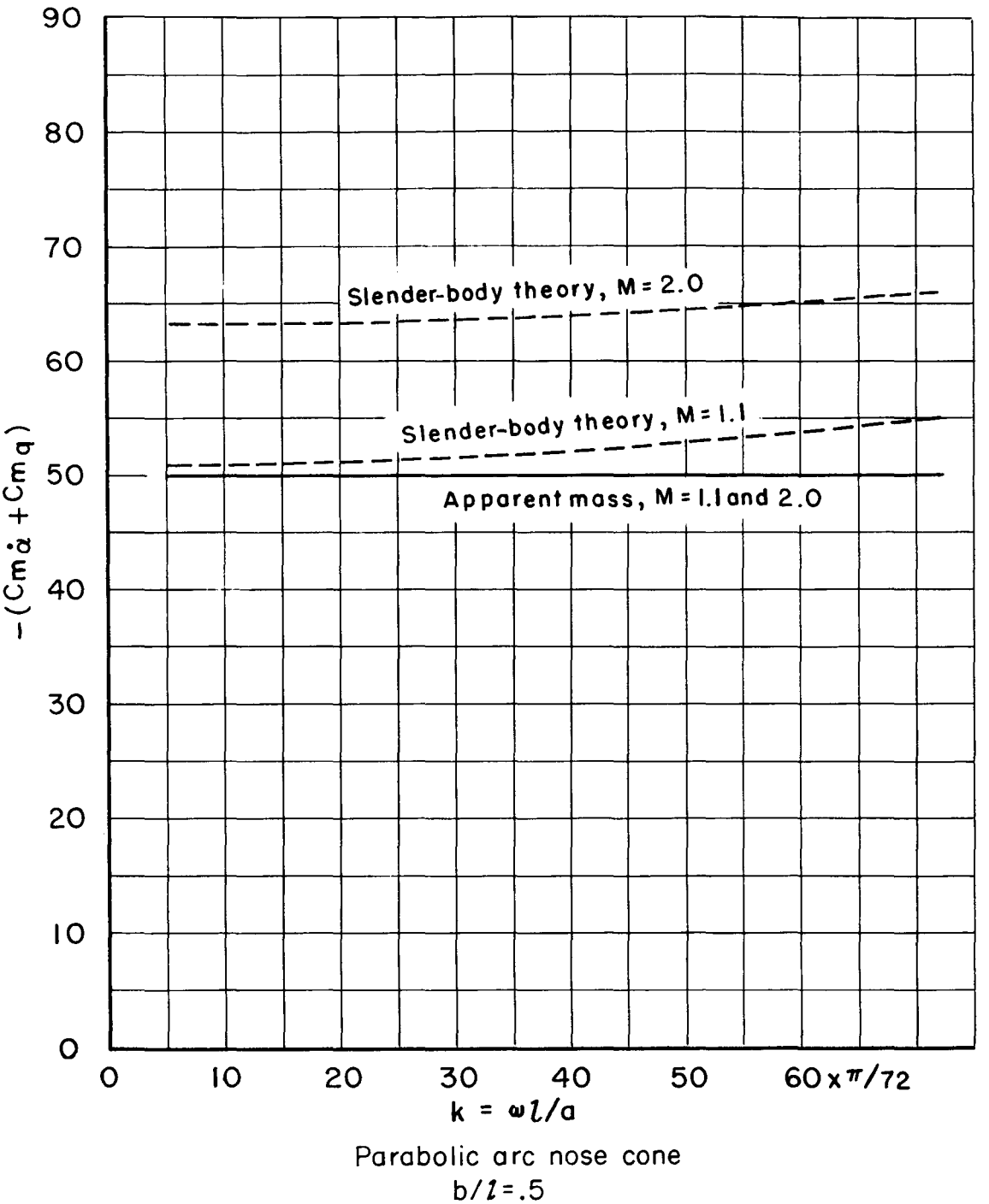

Figure 8.- Effect of increasing frequency on $C_{m_{\dot{\alpha}}} + C_{m_q}$.

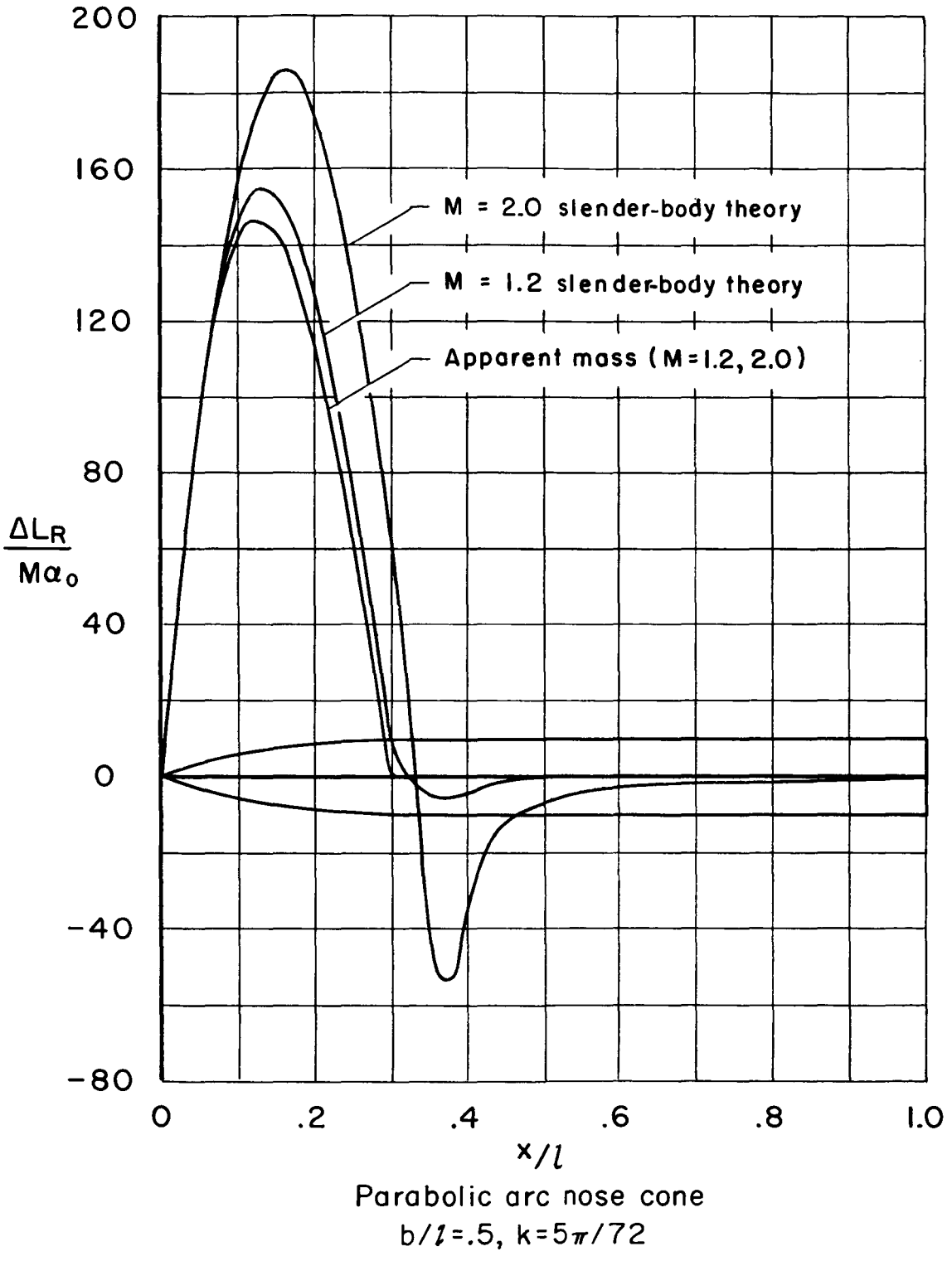

Figure 9.- Comparison of real part of local lift for M = 1.2 and M = 2.0.

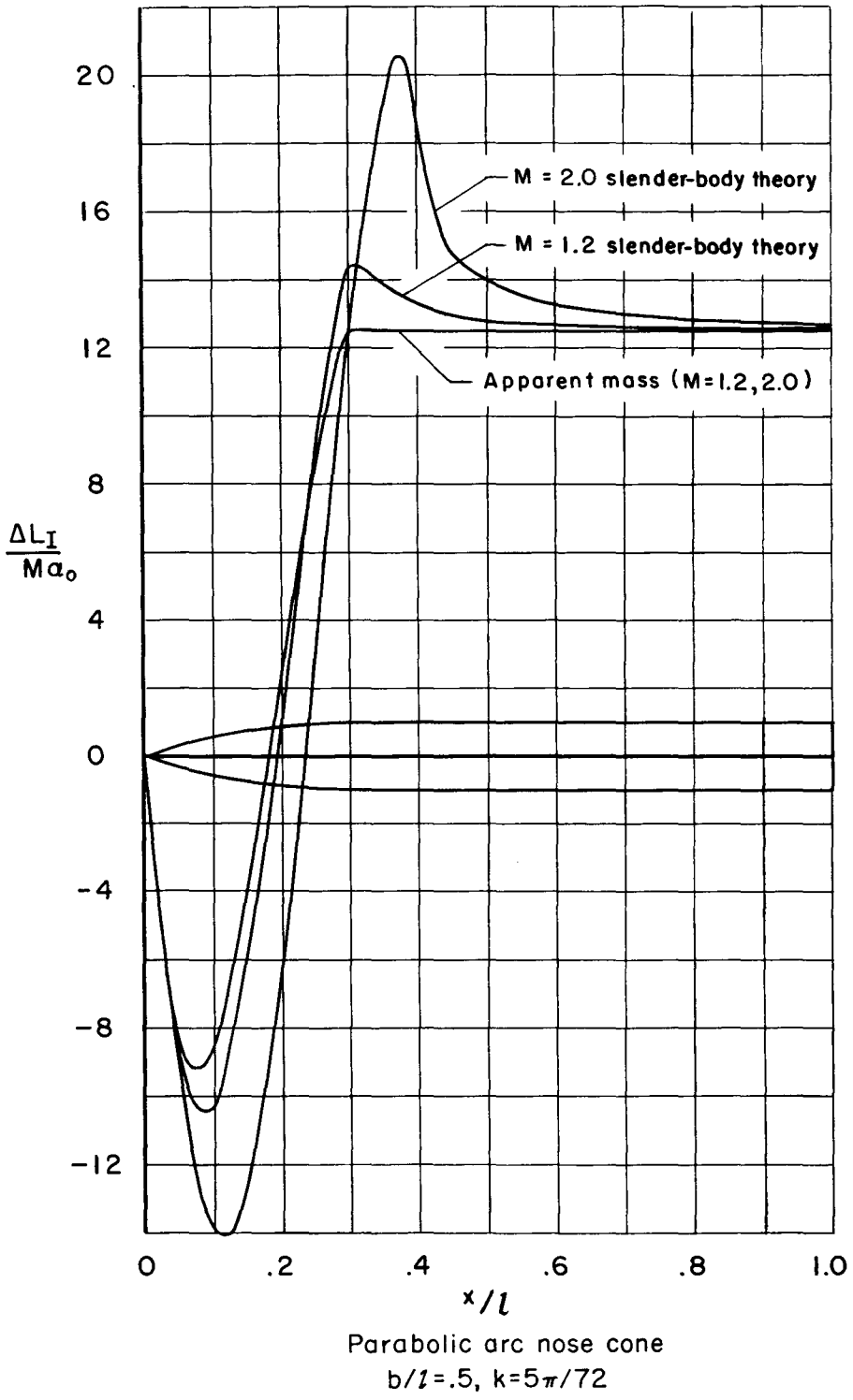

Figure 10.- Comparison of imaginary part of local lift for M = 1.2 and M = 2.0.